ARTICLE
Journal of Cellular Biochemistry 108:125–133 (2009)

Journal of Cellular Biochemistry

Matrin 3: Chromosomal Distribution and Protein Interactions

Michael J. Zeitz, Kishore S. Malyavantham, Brandon Seifert, and Ronald Berezney*

Department of Biological Sciences, University at Buffalo, State University of New York, Buffalo, New York 14260

ABSTRACT

Matrin 3 (matr3), an abundant protein of the internal nuclear matrix, has been linked to a variety of functional events. As a step toward defining its multifunctional nature, we have studied the association of matr3 with chromosome territories and identified potential interacting proteins. A similar staining pattern of matr3 was observed in fixed WI38 fibroblast cells and in live HeLa cells using a matr3-GFP construct. Matr3 was detected throughout autosomal and the active X chromosome territories. Conversely, matr3 was strikingly excluded from the inactive X chromosome as well as within both the perinuclear and perinucleolar heterochromatin. Yeast two hybrid analysis identified matr3 interactions with 33 unique nuclear localized proteins and also revealed its propensity for self association. A majority of these proteins are involved in RNA metabolism and chromatin remodeling while others function in protein translation, DNA replication/repair and apoptosis. Further analysis of a selection of these proteins and scaffold attachment factor A (SAFA) by co-localization and co-immunoprecipitation experiments using HeLa cells confirmed their interactions with matr3. J. Cell. Biochem. 108: 125–133, 2009.

KEY WORDS: NUCLEAR MATRIX; CHROMOSOME TERRITORIES; FLUORESCENCE IN SITU HYBRIDIZATION; MATRIN 3

An emerging view of the nucleus is that of a heterogeneous organelle partitioned into dynamic functional sub-domains or microenvironments throughout the three-dimensional nuclear volume [Wei et al., 1998; Berezney, 2002; Stein et al., 2003; Zaidi et al., 2005; Lanctot et al., 2007; Misteli, 2007; Malyavantham et al., 2008b]. The nuclear matrix consists of a fibrogranular framework of the interphase nucleus, which is resistant to high salt and detergent extraction [Berezney and Coffey, 1977; He et al., 1990] and has been proposed to contribute to the spatial and functional organization of the nucleus [Berezney, 2002]. Numerous functions including, but not limited to DNA replication, transcription, RNA splicing, and nuclear receptor signaling have been found associated with components of the nuclear matrix [Tubo et al., 1987; Zeitlin et al., 1987; Berezney et al., 1995; Mortillaro et al., 1996; Eggert et al., 1997; Oesterreich et al., 2000; Graham et al., 2008]. Many groups have identified specialized functional domains within the interphase nucleus [Lamond and Earnshaw, 1998; Dundr and Misteli, 2001; Zaidi et al., 2005]. Recently, we have demonstrated the presence of the nuclear matrix proteins matrin 3 (matr3) and scaffold attachment factor A (SAFA) also known as hnRNP-U in transcription-associated nuclear microenvironments [Malyavantham et al., 2008b]. Matr3, an abundant protein of the internal nuclear matrix [Belgrader et al., 1991; Nakayasu and Berezney, 1991], was originally cloned from a rat insuloma cDNA library [Belgrader et al., 1991]. Matr3 has since been implicated in processes such as nuclear retention of hyper-edited RNA [Zhang and Carmichael, 2001], and mediating neuronal cell death in response to NMDA receptor activation [Giordano et al., 2005].

SAFA, another abundant protein of the nuclear matrix, has been demonstrated to stabilize specific mRNAs [Yugami et al., 2007]. There is also evidence that SAFA plays a role in active transcription through an interaction with actin and RNA polymerase II [Kukalev et al., 2005; Obrdlik et al., 2008]. Both matr3 and SAFA have been demonstrated to bind DNA at sites termed scaffold/matrix attachment regions (S/MAR) [Fackelmayer et al., 1994; Gohring and Fackelmayer, 1997; Hibino et al., 2000]. S/MAR sites have been demonstrated to influence higher order chromatin structure by associating with matrix-binding proteins that anchor chromatin into loop domains [Cai et al., 2003]. The interplay of S/MAR sites and associated proteins can alter the structure of these chromatin loop domains to regulate gene expression [Cai et al., 2003; Heng et al., 2004; Han et al., 2008; Ottaviani et al., 2008]. In agreement with

Additional Supporting Information may be found in the online version of this article.

Grant sponsor: NIH; Grant number: GM 072131.

Michael J. Zeitz's present address is Stanford Medical School, 3801 Miranda Avenue, Palo Alto, CA 94304.

Kishore S. Malyavantham's present address is IMMCO Diagnostics Ltd, 60 Pine View Drive, Buffalo, NY 14228.

*Correspondence to: Ronald Berezney, Department of Biological Sciences, University at Buffalo, State University of New York, Buffalo, NY 14260. E-mail: berezney@buffalo.edu

Received 5 May 2009; Accepted 6 May 2009 • DOI 10.1002/jcb.22234 • © 2009 Wiley-Liss, Inc.

Published online 26 June 2009 in Wiley InterScience (www.interscience.wiley.com).

studies suggesting a role for the nuclear matrix in organizing chromatin structure, our group has previously demonstrated that disruption of a sub-set of nuclear matrix proteins is correlated with a loss of chromosome territory integrity [Ma et al., 1999].

In this report, we investigate the nuclear organization of matr3 with respect to interphase chromosomes. Using a combination of immunofluorescent staining and fluorescence in situ hybridization termed *immuno-FISH*, we demonstrate the ubiquitous nature of matr3 localization throughout autosomal chromosome territories and the exclusion of matr3 from the inactive X chromosome. Moreover, the network-like organization of matr3 visualized in fixed cells is also seen in live cells using a matr3–GFP construct. As a step toward understanding the functional role of matr3, a yeast two-hybrid screen was performed to identify candidate interacting proteins. Co-localization analysis and co-immunoprecipitation of matr3 with the candidate interacting proteins, scaffold attachment factor B (SAFB) and heterogeneous nuclear ribonucleoprotein L (hnRNP-L), with the addition of SAFA based on our previous findings [Malyavantham et al., 2008b] was conducted to verify the interactions in human cells.

MATERIALS AND METHODS

CELL CULTURE

HeLa and WI38 human diploid fibroblast cell lines (ATCC, Rockville, MD) were cultured in advanced DMEM containing 3% FBS, 1% penicillin, and streptomycin in a 37°C incubator at 5% CO_2.

MATR3–GFP CONSTRUCTION, TRANSFECTION, AND MICROSCOPY

The full-length open-reading frame of Matr3 (GenBank Number: BC015031; I.M.A.G.E. Clone ID: 3921668) was amplified from a pCMV-SPORT6 cDNA clone using suitable forward and reverse primers and topo-cloned into a pcDNA3.1/NT-GFP-TOPO vector according to the instructions provided by the NT-GFP Fusion TOPO® TA Expression Kit (Invitrogen, La Jolla, CA; catalog no. K4810-01). The fusion construct was transfected into HeLa cells using Lipofectamine and Plus reagents according to the manufacturer's recommendation (Invitrogen, La Jolla). HeLa cells expressing N-terminal GFP-fused Matr3 were imaged 24–36 h after transfection using an Olympus IX70 inverted fluorescence microscope.

YEAST TWO HYBRID

Full-length matr3 was PCR amplified from human cDNA with primers incorporating a *Bam*HI and a *Pst*I restriction site on the 5′ and 3′ ends, respectively. Matr3 cDNA was then double digested with *Bam*HI and *Pst*I (Fermentas) and the resulting fragment separated by agarose gel electrophoresis and isolated with a gel purification column (Qiagen). Matr3 was then cloned into plasmid pGBDU-C [James et al., 1996] containing the GAL4 DNA-binding domain generating pGBDU-Cmatr3. Plasmid pGBDU-Cmatr3 was transformed into yeast strain PJ69-4A [James et al., 1996] using polyethylene glycol/lithium acetate (PEG/LiAc)-mediated transformation [Gietz et al., 1992] and checked for expression and to rule out autoactivation on SD/-Ade and SD/-His plates. A full-length human fetal brain cDNA library in vector pACT2 (Clontech) was then transformed into PJ69-4A yeast expressing matr3 using a (PEG/LiAc) large-scale transformation method according to manufacturer's instructions (Clontech). Yeast transformants were plated for screening onto SD/-Ade/-His/-Ura/-Leu media. Selected colonies were patched to SD/-Leu plates and pGBDU-Cmatr3 was removed with 5′-FOA treatment. Candidate interacting clones were rescued from yeast and electroporated into Electromax DH10B cells (Invitrogen). Plasmids were isolated from the resulting colonies and sequenced at the DNA sequencing facility at Roswell Park Cancer Institute.

ANTIBODIES AND IMMUNOFLUORESCENCE

Primary antibodies used were rabbit polyclonal antibody against matr3 (clone BL2526, Bethyl Laboratories, Inc., Montgomery, TX), mouse monoclonal antibodies against hnRNP-U (clone 3G6), and hnRNP-L (clone 4D11) and goat polyclonal antibodies against SAFB, clone F20, (Santa Cruz Biotechnology, Santa Cruz, CA). Alexa488, Alexa594, and Alexa647 conjugated anti-goat, anti-mouse, and anti-rabbit secondary antibodies were purchased from Molecular Probes, Invitrogen (Carlsbad, CA). Peroxidase conjugated bovine anti-goat IgG was obtained from Jackson ImmunoResearch Laboratories (West Grove, PA), while peroxidase conjugated goat anti-mouse and goat anti-rabbit antibodies were from Sigma (St. Louis, MO).

For immuno-labeling, the cells grown on cover slips were fixed with 4% PFA/1× PBS for 10 min, made permeable by incubating in 0.5% Triton X-100 for 10 min at room temperature, and reacted with the appropriate primary antibody (diluted 1:100 in 10% FBS) for 1 h at room temperature. Cells were then washed twice in 1× PBS/0.1% Tween-20 (PBST) for 15 min at 37°C, labeled for 1 h (room temperature) with secondary antibodies diluted (1:200) in 1× PBS, washed twice in PBST for 15 min at 37°C and the cover slips mounted on slides using vectashield (Vector Laboratories, Burlingame, CA). Nuclei were detected with DAPI stain.

A modified labeling protocol was employed to eliminate antibody cross-reactivity when combining anti-rabbit and anti-goat secondary antibodies. Following primary antibody incubations, donkey anti-goat Alexa594 was labeled, washed with PBST, and fixed in place with 2% PFA/1× PBS for 5 min. Cells were then washed with 0.2% Triton X-100/1× PBS for 5 min followed by incubation with goat anti-rabbit Alexa488.

THREE-DIMENSIONAL IMMUNO-FISH

For DNA FISH, cells were fixed with 4% PFA/1× PBS for 10 min, made permeable with 0.5% Triton X-100 for 10 min, and incubated in 20% glycerol/1× PBS for 25 min followed by four freeze–thaw cycles in liquid nitrogen. Cells were heat denatured in 70% formamide/2× SSC at 75°C for 5 min followed immediately by denaturation in 50% formamide/2× SSC at 75°C for 2 min. Chromosome paints (Cytocell, Windsor, CT) were heat denatured at 75°C for 8 min and snap cooled on ice. Cells on cover slips were sealed together with chromosome paints using rubber cement, and chromosomes were hybridized for 24–48 h at 37°C. Three

post-hybridization washes included 50% formamide/2× SSC/0.05% Tween-20, 2× SSC/0.05% Tween-20, and 1× SSC for 30 min each at 37°C. Following the washes, cells were incubated with primary anti-matr3 antibody and secondary Alexa conjugated antibodies as described above. The cover slips were then mounted with vectashield. At no time were the cells allowed to dry.

CO-IMMUNOPRECIPITATION AND WESTERN BLOTTING

Co-immunoprecipitation of matr3 was performed with a nuclear complex Co-IP kit (Active Motif, Carlsbad, CA), according to manufacturer's instructions with minor modifications. Briefly, isolated HeLa nuclei were lysed in digestion buffer and DNA was digested with an enzymatic shearing cocktail in the presence of a protease inhibitor cocktail and PMSF. Four hundred micrograms of nuclear extract diluted in high stringency IP buffer was incubated on a rotator overnight at 4°C with 4 μg rabbit anti-matr3 or non-specific rabbit IgG (Sigma) in the case of the negative control. Extracts were then incubated with 60 μl of protein A magnetic Dynabeads (Invitrogen, Carlsbad), for 45 min at 4°C followed by three washes in IP wash buffer containing 1 mg/ml BSA and three washes in IP wash buffer alone. Complexes were removed from beads by boiling for 5 min in 10 μl of 2× SDS sample buffer.

Protein samples were separated by SDS–PAGE on 4–20% gradient ready gels (BioRad, Hercules, CA). Proteins were then transferred to a PVDF membrane (Millipore, Billerica, MA), and blocked overnight in 4% BSA and immunolabeled with primary antibodies followed by peroxidase conjugated secondary antibodies. Signals were detected using the ECL plus reagent (GE Healthcare, Piscataway, NJ), on a Storm860 imager (Molecular Dynamics, GE healthcare), according to manufacturer's recommendations.

MICROSCOPY AND COMPUTER IMAGE ANALYSIS

Following labeling, indirect immunofluorescence was detected with Chroma filter sets using an Olympus BX51 upright microscope (100× plan-apo, oil, 1.4 NA) equipped with a Sensicam QE (Cooke Corporation, Romulus, MI), digital CCD (charge-coupled device) camera, motorized *z*-axis controller (Prior, Rockland, MA), and Slidebook 4.0 software (Intelligent Imaging Innovations, Denver, CO). Optical sections (0.5 μm) were collected, deconvolved using a NoNeighbor algorithm operating within Slidebook 4.0, and exported as 16-bit tiff intensity files for further analysis. The matr3 sites were segmented according to a spot-based approach developed by our group [Malyavantham et al., 2008a,b]. The minimal spanning tree (MST) algorithm was then applied to the centroids of the segmented sites in order to evaluate the network-like properties of the matr3 sites [Malyavantham et al., 2008b]. Three-dimensional edge detection was performed with Slidebook 4.0 software.

To verify the accuracy of our co-localization studies, we imaged 0.5 μm diameter Fluoresbrite beads (Polysciences, Inc. Warrington, PA) in both the red and green channels and examined the merged images. Observation of completely yellow beads confirmed the overall validity of our results. We further determined that the average sub-pixel shift between the red and green channels of the imaged beads was 0.54 pixels (~0.03 μm) under the microscopic conditions used in our experiments [Malyavantham et al., 2008a].

Confocal microscopy was performed with a Zeiss LSM 510 Meta NLO confocal microscope at the confocal microscopy and flow cytometry core facility at the University at Buffalo. Confocal images were processed and orthogonal section views were displayed using LSM Image Browser (Zeiss, Thornwood, NY).

RESULTS

SPATIAL ORGANIZATION OF Matr3 AND CHROMOSOME TERRITORIES

Nuclear matrix proteins bind DNA at multiple sites in the genome termed S/MAR [Bidwell et al., 1993; Nayler et al., 1998; Cai et al., 2006]. Extraction of large portions of nuclear matrix proteins from the cell nucleus correlates with a significant disruption of three-dimensional chromosome territory organization [Ma et al., 1999]. Since matr3 is among the most abundant proteins identified in the inner nuclear matrix [Nakayasu and Berezney, 1991], we investigated its relationship with interphase chromosome territories.

Matr3 is localized throughout the extranucleolar regions of the nucleus and was composed of relatively discrete sites of varying intensities and more diffuse labeling (Fig. 1) that overall appears as a network-like structure [Malyavantham et al., 2008b]. The discrete matr3 sites are more easily distinguished at higher magnification (see insets in Fig. 1A,B). A similar organization of matr3 appears in live HeLa cells that were transfected with a matr3–GFP construct (Fig. 1I). To better evaluate the network-like properties of the matr3-staining patterns, we applied the MST algorithm to the centroids (visualize as red spots in Fig. 1I). This pattern recognition imaging approach connects the centroids by a line path that follows properties of both the nearest distance between the centroids and a minimal distance for the entire pathway of the continuous MST line [Malyavantham et al., 2008b]. This is seen in Figure 1J where the network-like green MST line is superimposed on the original raw image of matr3 staining.

An immuno-FISH approach was used to determine the spatial organization of matr3 in relationship to chromosome territories. Three-dimensional FISH was performed to preserve nuclear structure followed by indirect immunofluorescent labeling of matr3. Matr3 was observed to innervate both gene-poor chromosome 18 and gene-rich chromosome 19 regions (Fig. 1A,B). While the intense staining of the chromosome territories often masked the presence of at least the lower intensity matr3 sites, this association was confirmed by line profile analysis of chromosomes 18, 19, and matr3 (Fig. 1K,L). As another approach to defining the association of matr3 with chromosome territories, we employed the MST algorithm to map the network structure of matr3 with respect to chromosomes 1 and 9. The resulting matr3–MST network in blue is readily seen to penetrate into the interior of both pairs of chromosome territories (Fig. 1D).

The association of matr3 sites with chromosome territories 1 and 9 was then studied using confocal microscopy (Fig. 1C). For a more detailed visualization of the penetration of matr3 throughout chromosomes 1 and 9, we obtained in addition to XY optical sections (Fig. 1C, middle box), XZ (Fig. 1C, top box), and YZ (Fig. 1C, right box) sections denoted by the green and red lines,

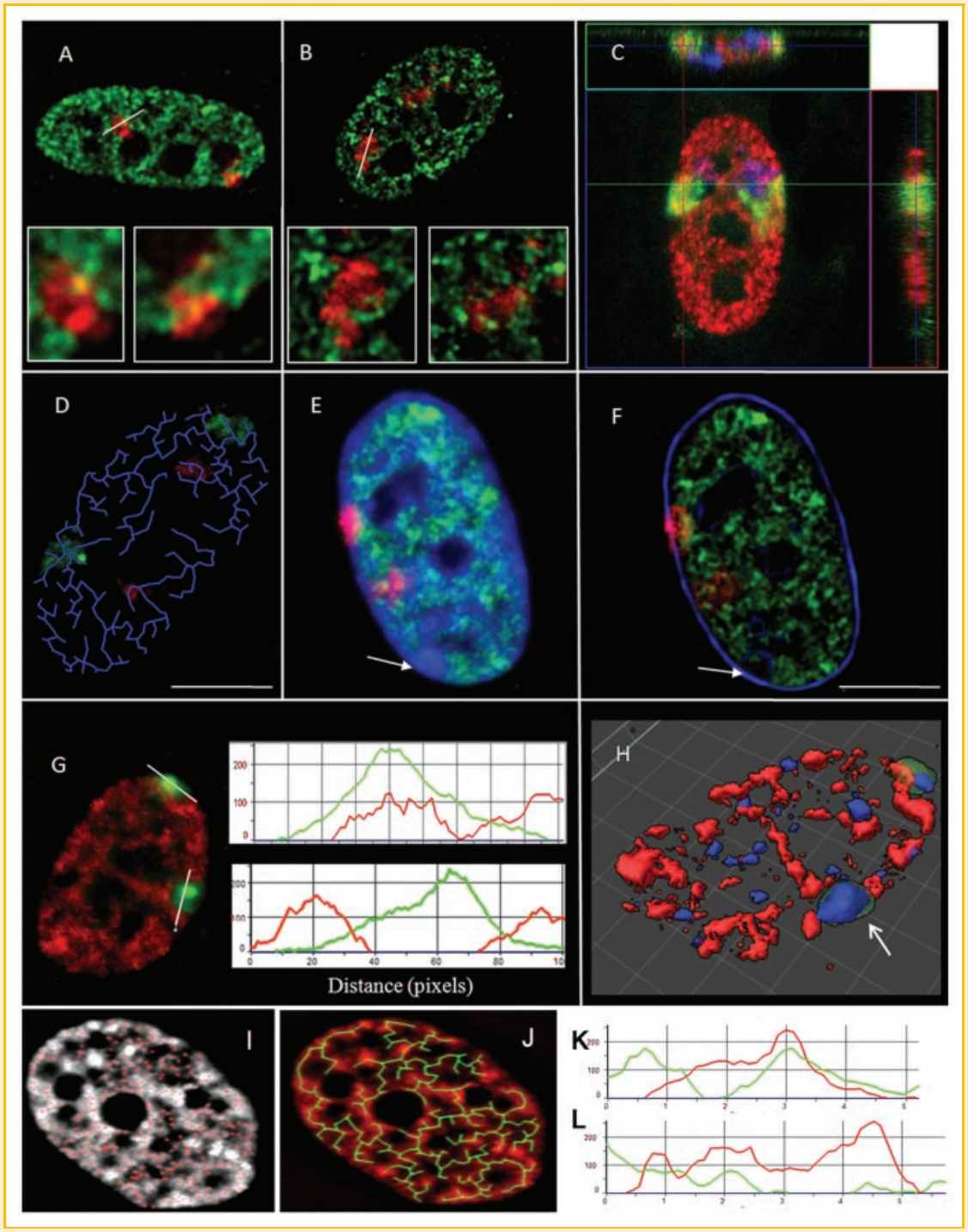

Fig. 1. Nuclear organization of Matr3 in WI38 fibroblasts and in live HeLa Cells. A: Matr3 (green) and chromosome 18 (red). B: Matr3 (green) and chromosome 19 (red). White boxes in (A) and (B) contain enlarged views of the chromosome territories and matr3. C: Confocal image displaying XY view (middle box), XZ section view (top box), and YZ section view (right box) of matr3 (red), chromosome 1 (green), and chromosome 9 (blue). D: Minimal spanning tree network of matr3 (blue lines), chromosome 1 (green), and chromosome 9 (red). E: Matr3 (green), chromosome 18 (red), and DAPI (blue). F: Three-dimensional edge detection analysis of the image from (E). Arrows in (E) and (F) denote the presumptive Barr body based on DAPI staining. G: Top, line profile analysis of active chromosome X and matr3 labeling; bottom, line profile of inactive X chromosome and matr3. H: Three-dimensional surface rendering of matr3 (red), X chromosome (green), and most intense DAPI staining (blue) White arrow denotes the inactive X chromosome. I: Distribution of matr3–GFP in live HeLa cells. Centroids (red) of discrete matr3 sites are superimposed on the raw image. J: MST network of the matr3–GFP sites (green) is overlaid on the raw matr3–GFP signal (red). K: Line profile of matr3 (green) and chromosome 18 (red) from (A). J: Line profile of matr3 (green) and chromosome 19 (red) from (B).

respectively. In the XY section only one copy of chromosome 9 is visible due to it occupying a different Z section. This is also the case for chromosome 1 in the YZ section.

The nuclear staining of matr3 excluded regions of heterochromatin as observed by regions of intense DAPI staining (Fig. 1E). To further test this conclusion, a three-dimensional edge detection algorithm was employed to precisely delineate the borders of DAPI-stained heterochromatin and matr3 staining (Fig. 1F). Matr3 is absent from both the perinuclear and perinucleolar heterochromatin. It also excludes the presumptive Barr body of the inactive X chromosome as suggested by the very intense and discrete region of DAPI staining along the nuclear periphery (Fig. 1F). Consistent with this interpretation, immuno-labeling of matr3 and the chromosome X paint revealed the absence of matr3 from one copy of the X chromosome (Fig. 1G) which is confirmed by line profile analysis (Fig. 2G). Three-dimensional surface rendering of chromosome X, matr3, and DAPI staining also supports the absence of matr3 from the intensely DAPI-stained heterochromatin of the inactive X chromosome but not the active X chromosome (Fig. 2H).

Matr3 INTERACTION SCREEN AND ANALYSIS OF ASSOCIATED PROTEINS

As an initial step toward understanding the functional interactions of matr3 in the cell nucleus, a yeast two-hybrid screen was performed to identify interacting proteins. Since matr3 expression is elevated in developing brain tissue, and is the main target for cAMP-dependent protein kinase (PKA) phosphorylation following NMDA receptor activation in neuronal cells [Giordano et al., 2005], a fetal brain cDNA library was used as prey. After screening greater than 2×10^6 colonies, 33 unique nuclear proteins were identified (Fig. 2). The great majority of these candidate interacting proteins were previously identified as playing functional roles in transcription, RNA processing/transport, and chromatin remodeling. The other proteins identified can be classified into the categories of DNA replication and repair, translation, and apoptosis. The most frequently found interactive protein was matr3 itself with six positive hits followed closely by the chromatin remodeling factor CHD3 and the RNA processing protein DDX5 with five hits each.

A combination of microscopy and co-immunoprecipitation was utilized to verify interactions of candidate proteins for which suitable antibodies were available. Two candidate proteins hnRNP-L, a global splicing regulator [Hung et al., 2008], and SAFB, a S/MAR-binding protein with roles in transcriptional repression [Nayler et al., 1998; Jiang et al., 2006], were analyzed for co-localization with matr3. SAFA was also included based on findings that it is highly proximal to matr3 by immuno-localization [Malyavantham et al., 2008b] and its proposed role in modulating RNA polymerase II transcription [Obrdlik et al., 2008]. All three proteins were observed to partially co-localize with matr3 (Fig. 3A–C). Both hnRNP-L and SAFB typically had concentrated regions of intense staining which co-localized completely with matr3 indicated by arrows in Figure 3A,C. These concentrated areas were often found proximal to nucleoli. To evaluate the degree of overlap between the candidate proteins and matr3, line profile analysis was performed (Fig. 3D–F). SAFA, SAFB, and hnRNP-L proteins displayed coincident peaks with matr3. SAFA distribution

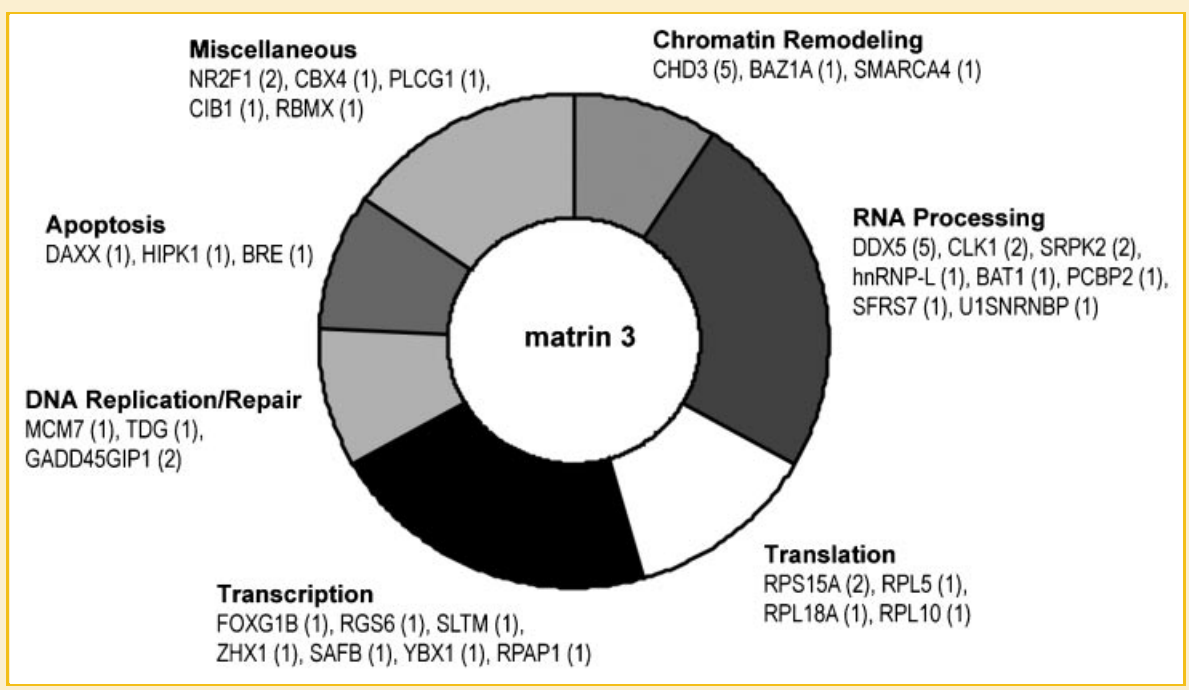

Fig. 2. Known nuclear proteins associating with matr3 from yeast two-hybrid analysis. Candidate interacting proteins from a yeast two-hybrid screen are broken into categories according to function. Numbers in parentheses indicate number of times interaction was found. Matr3 was found to associate with itself six times.

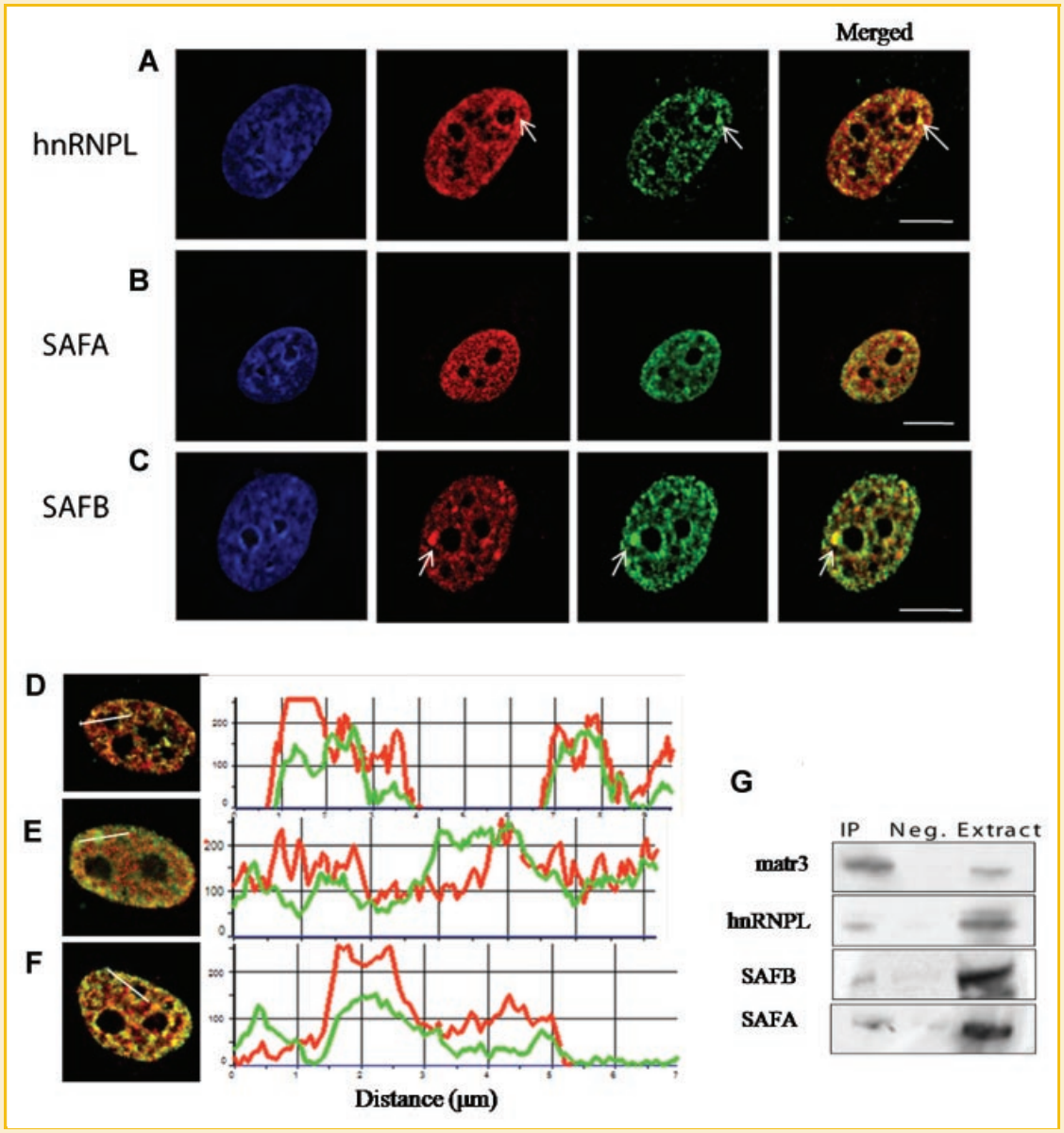

Fig. 3. Immunofluorescence and immuno-pulldown experiments of matr3 with hnRNP-L, SAFA, and SAFB. Analysis of matr3 and candidate interacting proteins in HeLa cells. A–C: Co-localization of matr3 (green) and (A) hnRNP-L (red), (B) SAFA (red), (C) SAFB (red), DAPI staining (blue), last column merged red and green images. White arrows in (A) and (C) denote co-localizing regions of intense matr3 staining. D–F: Line profile analysis of (D) matr3 (green) and hnRNP-L (red), (E) matr3 (red) and SAFB (green), (F) matr3 (red) and SAFA (green). G: Co-immunoprecipitation of matr3. Matr3 was immunoprecipitated from HeLa cell lysates, and the interacting proteins were detected by Western blot analysis. Lanes from left to right: IP, immunoprecipitation of matr3; neg., negative control immunoprecipitation with non-specific rabbit IgG; extract, total HeLa cell lysate run on the Western blot.

was more punctuate than matr3 and can be seen as multiple red peaks along the underlying matr3 line intensity profile (Fig. 3E). The line profiles also confirm that all three proteins are excluded from the interior of the nucleolus.

Additional candidate proteins brg1, a component of matrix-associated ATP-dependent chromatin remodeling complexes [Reyes et al., 1997], and the RNA-binding protein hnRNP-G were also investigated for co-localization with matr3 (Supplementary Fig. S1). Although both proteins displayed partial co-localization with matr3 (Supplementary Fig. S1) they were not detected in co-immunoprecipitation experiments under the conditions employed (data not shown).

Nuclear co-immunoprecipitation experiments were performed to determine if the close associations found between matr3 and hnRNP-L, SAFB and SAFA by immunofluorescence microscopy reflect actual protein interactions with matr3. Prior to immunoprecipitation, a nuclease cocktail was used to release DNA bound proteins from isolated HeLa nuclei. Endogenous matr3 was then immunoprecipitated from the HeLa cell nuclear extracts. Immunoblotting revealed the presence of SAFA, SAFB, and

hnRNP-L in the fraction pulled down with matr3 but not in the fraction pulled down with non-specific rabbit IgG antibodies (Fig. 3G).

DISCUSSION

The nuclear matrix has long been thought to organize the myriad of processes occurring in the cell nucleus [Berezney and Coffey, 1977; Berezney, 1984; Berezney et al., 1995]. The more recent findings of spatial organization and the identification of numerous heterogeneous functional domains support this hypothesis [Berezney, 2002; Stein et al., 2003; Zaidi et al., 2005; Misteli, 2007; Malyavantham et al., 2008b]. Nearly all nuclear processes examined to date have been found associated with nuclear matrix components [Tubo et al., 1987; Zeitlin et al., 1987; Bidwell et al., 1993; Berezney et al., 1995; Oesterreich et al., 2000; Graham et al., 2008]. In addition to nuclear matrix associations with functional processes, a role is also suggested in organizing higher order chromatin structure through S/MAR binding [Heng et al., 2004; Cai et al., 2006; Ottaviani et al., 2008]. This hypothesis is furthered by the observation of chromosome territory disruption in correlation with the corresponding disruption of nuclear matrix structure in permeabilized cells [Ma et al., 1999].

Although association with the nuclear matrix has been widely demonstrated for many nuclear processes, the exact function of many nuclear matrix proteins remains unclear. Progress has been made, however, in the analysis of matr3, one of the more abundant proteins of the internal nuclear matrix [Nakayasu and Berezney, 1991]. It has been linked to a variety of nuclear processes including retention of hyper-edited RNA within the nucleus [Zhang and Carmichael, 2001] and neuronal degradation in response to NMDA activation [Giordano et al., 2005]. In the case of nuclear RNA retention, matr3 was found to isolate in a complex with p54(nrb), and the polypyrimidine tract binding protein associated splicing factor (PSF), formally known as matrin 4 [Zhang and Carmichael, 2001]. There is difficulty explaining the difference in the number of reported amino acids at 876 in the report by Carmichael's group.

With this as a basis, we have investigated the nuclear organization of matr3 in relationship to the chromosome territories, followed by identification of potential interacting protein factors within the cell nucleus. Matr3 foci varied in intensity from very bright to weak and were distributed throughout the interphase nucleus. While many sites occurred proximal to nucleoli, no significant staining was detected within the nucleolar interior. In the several hundred images observed, matr3 staining was present throughout each autosomal chromosome territory analyzed. No preference for increased matr3 localization was detected within either the gene-poor chromosome 18 or gene-rich chromosome 19 territories (Fig. 1A,B). Matr3 also was found to penetrate into chromosomes 1 and 9 territories when observed by three-dimensional confocal microscopy (Fig. 1C), and two-dimensional MST analysis of the matr3 foci yielded a network that innervated both chromosomes 1 and 9 (Fig. 1D). This network distribution is consistent with the finding that matr3 had a tendency to self-associate as evident from the yeast two-hybrid analysis. Importantly, a similar staining pattern and organization was detected in living HeLa cells using a matr3–GFP construct (Fig. 1I,J) These observations are also consistent with a model of chromosome territories that contains a network of interconnecting channels accessible to nuclear factors [Albiez et al., 2006]. Staining of matr3 was also largely excluded from regions rich in heterochromatic DNA including that of the inactive X chromosome (Fig. 1E–H) suggesting a possible role in euchromatin organization and/or function.

In an attempt to elucidate the functional interactions of matr3, we performed a yeast two-hybrid screen. Consistent with a euchromatic spatial location, the majority of positive interactions with matr3 contained proteins with a function involving transcription, RNA processing/transport, and chromatin remodeling (Fig. 2). There were also interactions with DNA replication/repair components including the replication origin binding factor MCM7 [Maiorano et al., 2006], and apoptosis-related proteins including the death-domain associated protein (DAXX), homeodomain interacting protein kinase 1 (HIPK1), and brain and reproductive organ-expressed protein (BRE). Interestingly, HIPK1 was observed to interact with DAXX and is proposed to modulate its activity and nuclear localization [Ecsedy et al., 2003]. There is also evidence that matr3, like numerous other nuclear matrix proteins, is susceptible to cleavage by caspases during apoptosis [Gerner et al., 2002; Valencia et al., 2007].

To examine the link between matr3 and RNA processing more closely, we performed co-localization and co-immunoprecipitation experiments with matr3 using HeLa cells. The nuclear protein hnRNP-L, which has been demonstrated to globally regulate RNA splicing [Hui et al., 2003; Hung et al., 2008], and the nuclear matrix protein SAFB1, which has been implicated in a variety of processes including chromatin organization and RNA processing [Oesterreich, 2003], were identified in the yeast two-hybrid screen and selected for further investigation. SAFA was also included based on its proximity to matr3 within functional nuclear domains [Malyavantham et al., 2008b] and its role in transcriptional regulation [Obrdlik et al., 2008]. We found significant overlap between matr3 foci and hnRNP-L, SAFA, and SAFB (Fig. 3A–C). This was further supported by the presence of coincident peaks observed from line profile analysis (Fig. 3D–F). In addition, hnRNP-L, SAFA, and SAFB were all identified in the fraction pulled down by immunoprecipitation of endogenous matr3. Together these data support the results from the yeast two-hybrid interaction screen and implicates a role for matr3 in RNA processing and structural organization.

Like many of the identified proteins of the nuclear matrix, matr3 has been observed to bind to S/MAR DNA [Hibino et al., 2000]. S/MAR DNA-binding proteins have been implicated in organizing chromatin loop domains and can display both activating and repressive influences on gene expression in a tissue-specific manner through interactions with chromatin remodeling and transcriptional machinery [Alvarez et al., 2000; Cai et al., 2003; Heng et al., 2004]. Although matr3 has been demonstrated to bind DNA, in vivo effects from its binding have not yet been determined. It would be interesting to compare global gene expression levels following siRNA-mediated knockdown of matr3 to assess whether it too functions to modulate transcriptional activity.

ACKNOWLEDGMENTS

We are grateful to Dr. Paul Cullen and Heather Dionne for providing advice in performing the yeast two-hybrid screen. Yeast strain PJ69-4A and plasmid pGBDU-C were gifts from Dr. Paul Cullen. This research was supported by NIH Grant GM 072131 awarded to R.B.

REFERENCES

Albiez H, Cremer M, Tiberi C, Vecchio L, Schermelleh L, Dittrich S, Kupper K, Joffe B, Thormeyer T, von Hase J, Yang S, Rohr K, Leonhardt H, Solovei I, Cremer C, Fakan S, Cremer T. 2006. Chromatin domains and the interchromatin compartment form structurally defined and functionally interacting nuclear networks. Chromosome Res 14:707–733.

Alvarez JD, Yasui DH, Niida H, Joh T, Loh DY, Kohwi-Shigematsu T. 2000. The MAR-binding protein SATB1 orchestrates temporal and spatial expression of multiple genes during T-cell development. Genes Dev 14:521–535.

Belgrader P, Dey R, Berezney R. 1991. Molecular cloning of matrin 3. A 125-kilodalton protein of the nuclear matrix contains an extensive acidic domain. J Biol Chem 266:9893–9899.

Berezney R. 1984. Organization and function of the nuclear matrix. In: Hnilica LS, editor. Chromosomal non-histone proteins—Structural associations. Boca Raton, FL: CRC Press. pp. 119–180.

Berezney R. 2002. Regulating the mammalian genome: The role of nuclear architecture. Adv Enzyme Regul 42:39–52.

Berezney R, Coffey DS. 1977. Nuclear matrix. Isolation and characterization of a framework structure from rat liver nuclei. J Cell Biol 73:616–637.

Berezney R, Mortillaro MJ, Ma H, Wei X, Samarabandu J. 1995. The nuclear matrix: A structural milieu for genomic function. Int Rev Cytol 162A:1–65.

Bidwell JP, Van Wijnen AJ, Fey EG, Dworetzky S, Penman S, Stein JL, Lian JB, Stein GS. 1993. Osteocalcin gene promoter-binding factors are tissue-specific nuclear matrix components. Proc Natl Acad Sci USA 90:3162–3166.

Cai S, Han HJ, Kohwi-Shigematsu T. 2003. Tissue-specific nuclear architecture and gene expression regulated by SATB1. Nat Genet 34:42–51.

Cai S, Lee CC, Kohwi-Shigematsu T. 2006. SATB1 packages densely looped, transcriptionally active chromatin for coordinated expression of cytokine genes. Nat Genet 38:1278–1288.

Dundr M, Misteli T. 2001. Functional architecture in the cell nucleus. Biochem J 356:297–310.

Ecsedy JA, Michaelson JS, Leder P. 2003. Homeodomain-interacting protein kinase 1 modulates Daxx localization, phosphorylation, and transcriptional activity. Mol Cell Biol 23:950–960.

Eggert M, Michel J, Schneider S, Bornfleth H, Baniahmad A, Fackelmayer FO, Schmidt S, Renkawitz R. 1997. The glucocorticoid receptor is associated with the RNA-binding nuclear matrix protein hnRNP U. J Biol Chem 272:28471–28478.

Fackelmayer FO, Dahm K, Renz A, Ramsperger U, Richter A. 1994. Nucleic-acid-binding properties of hnRNP-U/SAF-A, a nuclear-matrix protein which binds DNA and RNA in vivo and in vitro. Eur J Biochem 221:749–757.

Gerner C, Gotzmann J, Frohwein U, Schamberger C, Ellinger A, Sauermann G. 2002. Proteome analysis of nuclear matrix proteins during apoptotic chromatin condensation. Cell Death Differ 9:671–681.

Gietz D, St Jean A, Woods RA, Schiestl RH. 1992. Improved method for high efficiency transformation of intact yeast cells. Nucleic Acids Res 20:1425.

Giordano G, Sanchez-Perez AM, Montoliu C, Berezney R, Malyavantham K, Costa LG, Calvete JJ, Felipo V. 2005. Activation of NMDA receptors induces protein kinase A-mediated phosphorylation and degradation of matrin 3. Blocking these effects prevents NMDA-induced neuronal death. J Neurochem 94:808–818.

Gohring F, Fackelmayer FO. 1997. The scaffold/matrix attachment region binding protein hnRNP-U (SAF-A) is directly bound to chromosomal DNA in vivo: A chemical cross-linking study. Biochemistry 36:8276–8283.

Graham JD, Hanson AR, Croft AJ, Fox AH, Clarke CL. 2008. Nuclear matrix binding is critical for progesterone receptor movement into nuclear foci. FASEB J 23(2):546–556.

Han HJ, Russo J, Kohwi Y, Kohwi-Shigematsu T. 2008. SATB1 reprogrammes gene expression to promote breast tumour growth and metastasis. Nature 452:187–193.

He DC, Nickerson JA, Penman S. 1990. Core filaments of the nuclear matrix. J Cell Biol 110:569–580.

Heng HH, Goetze S, Ye CJ, Liu G, Stevens JB, Bremer SW, Wykes SM, Bode J, Krawetz SA. 2004. Chromatin loops are selectively anchored using scaffold/matrix-attachment regions. J Cell Sci 117:999–1008.

Hibino Y, Ohzeki H, Sugano N, Hiraga K. 2000. Transcription modulation by a rat nuclear scaffold protein, P130, and a rat highly repetitive DNA component or various types of animal and plant matrix or scaffold attachment regions. Biochem Biophys Res Commun 279:282–287.

Hui J, Stangl K, Lane WS, Bindereif A. 2003. HnRNP L stimulates splicing of the eNOS gene by binding to variable-length CA repeats. Nat Struct Biol 10:33–37.

Hung LH, Heiner M, Hui J, Schreiner S, Benes V, Bindereif A. 2008. Diverse roles of hnRNP L in mammalian mRNA processing: A combined microarray and RNAi analysis. RNA 14:284–296.

James P, Halladay J, Craig EA. 1996. Genomic libraries and a host strain designed for highly efficient two-hybrid selection in yeast. Genetics 144:1425–1436.

Jiang S, Meyer R, Kang K, Osborne CK, Wong J, Oesterreich S. 2006. Scaffold attachment factor SAFB1 suppresses estrogen receptor alpha-mediated transcription in part via interaction with nuclear receptor corepressor. Mol Endocrinol 20:311–320.

Kukalev A, Nord Y, Palmberg C, Bergman T, Percipalle P. 2005. Actin and hnRNP U cooperate for productive transcription by RNA polymerase II. Nat Struct Mol Biol 12:238–244.

Lamond AI, Earnshaw WC. 1998. Structure and function in the nucleus. Science 280:547–553.

Lanctot C, Cheutin T, Cremer M, Cavalli G, Cremer T. 2007. Dynamic genome architecture in the nuclear space: Regulation of gene expression in three dimensions. Nat Rev Genet 8:104–115.

Ma H, Siegel AJ, Berezney R. 1999. Association of chromosome territories with the nuclear matrix. Disruption of human chromosome territories correlates with the release of a subset of nuclear matrix proteins. J Cell Biol 146:531–542.

Maiorano D, Lutzmann M, Mechali M. 2006. MCM proteins and DNA replication. Curr Opin Cell Biol 18:130–136.

Malyavantham KS, Bhattacharya S, Alonso WD, Acharya R, Berezney R. 2008a. Spatio-temporal dynamics of replication and transcription sites in the mammalian cell nucleus. Chromosoma 117(6):553–567.

Malyavantham KS, Bhattacharya S, Barbeitos M, Mukherjee L, Xu J, Fackelmayer FO, Berezney R. 2008b. Identifying functional neighborhoods within the cell nucleus: Proximity analysis of early S-phase replicating chromatin domains to sites of transcription, RNA polymerase II, HP1gamma, matrin 3 and SAF-A. J Cell Biochem 105:391–403.

Misteli T. 2007. Beyond the sequence: Cellular organization of genome function. Cell 128:787–800.

Mortillaro MJ, Blencowe BJ, Wei X, Nakayasu H, Du L, Warren SL, Sharp PA, Berezney R. 1996. A hyperphosphorylated form of the large subunit of RNA polymerase II is associated with splicing complexes and the nuclear matrix. Proc Natl Acad Sci USA 93:8253–8257.

Nakayasu H, Berezney R. 1991. Nuclear matrins: Identification of the major nuclear matrix proteins. Proc Natl Acad Sci USA 88:10312–10316.

Nayler O, Stratling W, Bourquin JP, Stagljar I, Lindemann L, Jasper H, Hartmann AM, Fackelmayer FO, Ullrich A, Stamm S. 1998. SAF-B protein couples transcription and pre-mRNA splicing to SAR/MAR elements. Nucleic Acids Res 26:3542–3549.

Obrdlik A, Kukalev A, Louvet E, Farrants AK, Caputo L, Percipalle P. 2008. The histone acetyltransferase PCAF associates with actin and hnRNP U for RNA polymerase II transcription. Mol Cell Biol 28:6342–6357.

Oesterreich S. 2003. Scaffold attachment factors SAFB1 and SAF B2: Innocent bystanders or critical players in breast tumorigenesis? J Cell Biochem 90:653–661.

Oesterreich S, Zhang Q, Hopp T, Fuqua SA, Michaelis M, Zhao HH, Davie JR, Osborne CK, Lee AV. 2000. Tamoxifen-bound estrogen receptor (ER) strongly interacts with the nuclear matrix protein HET/SAF-B, a novel inhibitor of ER-mediated transactivation. Mol Endocrinol 14:369–381.

Ottaviani D, Lever E, Mitter R, Jones T, Forshew T, Christova R, Tomazou EM, Rakyan VK, Krawetz SA, Platts AE, Segarane B, Beck S, Sheer D. 2008. Reconfiguration of genomic anchors upon transcriptional activation of the human major histocompatibility complex. Genome Res 18:1778–1786.

Reyes JC, Muchardt C, Yaniv M. 1997. Components of the human SWI/SNF complex are enriched in active chromatin and are associated with the nuclear matrix. J Cell Biol 137:263–274.

Stein GS, Zaidi SK, Braastad CD, Montecino M, van Wijnen AJ, Choi JY, Stein JL, Lian JB, Javed A. 2003. Functional architecture of the nucleus: Organizing the regulatory machinery for gene expression, replication and repair. Trends Cell Biol 13:584–592.

Tubo RA, Martelli AM, Berezney R. 1987. Enhanced processivity of nuclear matrix bound DNA polymerase alpha from regenerating rat liver. Biochemistry 26:5710–5718.

Valencia CA, Ju W, Liu R. 2007. Matrin 3 is a Ca2+/calmodulin-binding protein cleaved by caspases. Biochem Biophys Res Commun 361:281–286.

Wei X, Samarabandu J, Devdhar RS, Siegel AJ, Acharya R, Berezney R. 1998. Segregation of transcription and replication sites into higher order domains. Science 281:1502–1506.

Yugami M, Kabe Y, Yamaguchi Y, Wada T, Handa H. 2007. hnRNP-U enhances the expression of specific genes by stabilizing mRNA. FEBS Lett 581:1–7.

Zaidi SK, Young DW, Choi JY, Pratap J, Javed A, Montecino M, Stein JL, van Wijnen AJ, Lian JB, Stein GS. 2005. The dynamic organization of gene-regulatory machinery in nuclear microenvironments. EMBO Rep 6:128–133.

Zeitlin S, Parent A, Silverstein S, Efstratiadis A. 1987. Pre-mRNA splicing and the nuclear matrix. Mol Cell Biol 7:111–120.

Zhang Z, Carmichael GG. 2001. The fate of dsRNA in the nucleus: A p54(nrb)-containing complex mediates the nuclear retention of promiscuously A-to-I edited RNAs. Cell 106:465–475.